THE JOURNAL OF PHYSICAL CHEMISTRY B

Article

pubs.acs.org/JPCB

Vapor–Liquid Equilibria of Imidazolium Ionic Liquids with Cyano Containing Anions with Water and Ethanol

Imran Khan,[†,§] Marta L. S. Batista,[†,§] Pedro J. Carvalho,[†] Luís M. N. B. F. Santos,[‡] José R. B. Gomes,[†] and João A. P. Coutinho*[,†]

[†]CICECO, Aveiro Institute of Materials, Chemistry Department, University of Aveiro, 3810-193 Aveiro, Portugal

[‡]Centro de Investigacão em Química, Departamento de Química e Bioquímica, Faculdade de Ciências da Universidade do Porto, Rua do Campo Alegre, 687, P-4169-007 Porto, Portugal

Supporting Information

ABSTRACT: Isobaric vapor–liquid equilibria of 1-butyl-3-methylimidazolium thiocyanate ($[C_4C_1im][SCN]$), 1-butyl-3-methylimidazolium dicyanamide ($[C_4C_1im][N(CN)_2]$), 1-butyl-3-methylimidazolium tricyanomethanide ($[C_4C_1im][C(CN)_3]$), and 1-ethyl-3-methylimidazolium tetracyanoborate ($[C_2C_1im][B(CN)_4]$), with water and ethanol were measured over the whole concentration range at 0.1, 0.07, and 0.05 MPa. Activity coefficients were estimated from the boiling temperatures of the binary systems, and the data were used to evaluate the ability of COSMO-RS for describing these molecular systems. Aiming at further understanding the molecular interactions on these systems, molecular dynamics (MD) simulations were performed. On the basis of the interpretation of the radial and spatial distribution functions along with coordination numbers obtained through MD simulations, the effect of the increase of CN-groups in the IL anion in its capability to establish hydrogen bonds with water and ethanol was evaluated. The results obtained suggest that, for both water and ethanol systems, the anion $[N(CN)_2]^-$ presents the higher ability to establish favorable interactions due to its charge, and that the ability of the anions to interact with the solvent, decreases with further increasing of the number of cyano groups in the anion. The ordering of the partial charges in the nitrogen atoms from the CN-groups in the anions agrees with the ordering obtained for VLE and activity coefficient data.

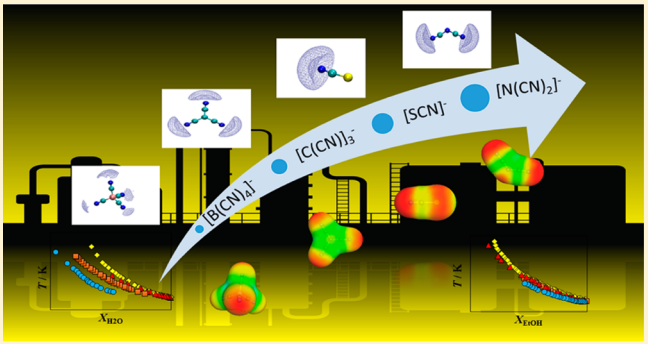

1. INTRODUCTION

The ethanol–water[1,2] system, found on the fermentation broth of the production of bioethanol, is of major economical relevance. It has been the subject of considerable number of studies[3] aiming at achieving an effective and economical separation process for the recovery of ethanol from the reacting media. In the field of separation processes, extractive distillation is the most common method for the separation of azeotropic or close-boiling mixtures. This process is based on the addition of another solvent, the entrainer, with high boiling point, that alters the relative volatility of the components enabling their separation.[3−5] The search for the best entrainer for the ethanol–water system has been the focus of attention of several research groups.[5−7] During the past decade, ionic liquids (ILs) have been studied as entrainers for extractive distillation having advantages over common organic compounds.[2,3,5] Ionic liquids possess unique properties, as for instance, good solvation capacity to dissolve a broad variety of compounds, a wide liquidus range, extremely low vapor pressures, and they are easy to recover and reuse. They are usually composed of large organic cations and inorganic or organic anions, with asymmetric structure and high charge dispersion at least on one of the ions. Through the combination of different cations and anions[8] it is possible to fine-tune their properties for specific applications, arising as suitable candidates to successfully replace common volatile organic compounds in different separation processes.[3−5,9]

The assessment of the applicability of an IL to act as entrainer in different azeotropic systems is usually made through vapor pressure, boiling temperature or through activity coefficient data. Vapor–liquid equilibria (VLE), along with activity coefficient data, allow the evaluation of the potential of excess Gibbs energy (G^E) models, widely used for the description of the nonideal behavior of these systems. Hence, the possibility of two-phase formation and the type/strength of the interactions established between IL and water/ethanol can be gauged and a separation process designed.[3,5,10]

Although object of interest during the past decade, limited research on VLE with ILs as entrainers for azeotropic separations has been reported.[5] Seiler et al.,[9] Jork et al.,[11] Beste et al.,[12] and Lei et al.[13] were among the first to show the use of ILs for separation of azeotropic mixtures. Revelli et al.[14]

Received: April 6, 2015
Revised: July 12, 2015
Published: July 13, 2015

DOI: 10.1021/acs.jpcb.5b03324
J. Phys. Chem. B 2015, 119, 10287−10303

Table 1. Structures of Investigated Ionic Liquids

Name and Abbreviation	Structure	
	Cation	Anion
1-butyl-3-methylimidazolium thiocyanate [C_4C_1im][SCN]	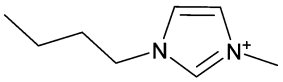	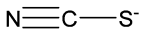
1-butyl-3-methylimidazolium dicyanamide [C_4C_1im][N(CN)$_2$]	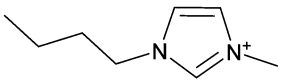	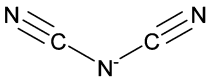
1-butyl-3-methylimidazolium tricyanomethanide [C_4C_1im][C(CN)$_3$]	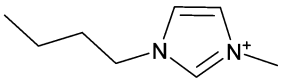	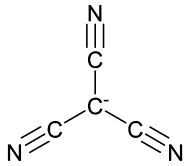
1-ethyl-3-methylimidazolium tetracyanoborate [C_2C_1im][B(CN)$_4$]	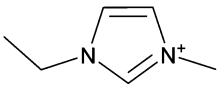	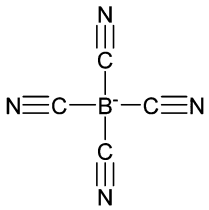

reported some binary mixtures containing imidazolium-based ILs with light alcohols. In the open literature, there are reports of several imidazolium-based ILs investigated for the extractive distillation of ethanol−water mixtures.[1,2,14−25] These studies focused on showing that the ILs may allow breaking the azeotrope, and on validating different procedures to measure VLE data with ILs. Ge et al.[1] and Orchillés et al.[24] compared and discussed the performance of the anions $[Cl]^-$, $[Ac]^-$, $[N(CN)_2]^-$, and $[BF_4]^-$ that they have been found to be the most suitable for an effective extractive distillation, according to the effect that they induce in the relative volatility of the system, which is also discussed in detail in the review of Pereiro et al.[5] The ILs with the anions $[Ac]^-$ and $[N(CN)_2]^-$ stand as the best candidates, not only due to their high propensity to interact favorably with water/ethanol, but also due to their lower viscosity (when comparing with the IL with the anion chloride) which enhance the mass transfer efficiency of the extractive distillation[26] or thermal stability when compared with $[BF_4]^-$.[27] The strong effect of water upon the viscosity of the ILs may further enhance this aspect and must be taken into account in the design of extraction processes.[28]

The experimental determination of VLE data, aiming at disclosing the ILs activity−structure relationship, is an impractical task if one takes into account the large number of potential ILs that can be prepared by the combination of available cations and anions. To overcome this difficulty, semiempirical group contribution models (such as UNIFAC[29]) and equations of state (such as PC-SAFT[18,30,31]) are commonly applied to correlate experimental data aiming at predicting other systems not previously studied, or predictive models such as COSMO-RS[10,32−35] have been used to scan the ILs in the quest for the best entrainers. Process simulators, such as Aspen Plus, can then be applied for an evaluation of the process and its optimization.[3,26]

Additionally, the use of molecular dynamics (MD) simulations has also been reported.[36,37] This computational approach based on statistical mechanic and Newton's equation of motion, allows the description of real systems at the atomic level, providing an understanding of the molecular interactions that take place.[38] This approach has the advantage of being capable to describe the dynamic behavior of systems, as well as, to predict its thermodynamic and transport properties.[39]

Regarding the large variety of ILs, cyano-based ILs present a set of properties of great interest like low melting points and low viscosities,[40] and a surprisingly wide hydrogen bond ability presenting themselves either as good solvents for carbohydrates (e.g., when the IL anion is $[N(CN)_2]^-$), or as water immiscible (e.g., when the IL anion is $[B(CN)_4]^-$). They have been studied for many specific applications, namely electrolytes and dye-sensitized solar cells,[41,42] extracting solvent for added-value compounds in biomass (phenolic compounds,[43] carbohydrates,[44,45] and sugar alcohols[46]) and aromatic−aliphatic separations[10] and were also shown to successfully extract alcohols from fermentation broth.[1,10,47]

In the present work, the binary systems composed of water or ethanol with imidazolium-based ILs, with anions containing an increasing number of CN-groups, were investigated. A systematic experimental study of the isobaric VLE, at pressures ranging from 0.05 to 0.1 MPa, along with the measurement of density and viscosity of the binary mixtures were performed. Additionally, COSMO-RS was evaluated on its ability to describe the studied systems and MD simulations were used

DOI: 10.1021/acs.jpcb.5b03324
J. Phys. Chem. B 2015, 119, 10287−10303

aiming at understanding the molecular level interactions responsible for the macroscopic phase behavior of these systems.

2. EXPERIMENTAL SECTION

2.1. Materials. Four imidazolium-based ILs with cyano containing anions were studied in this work, namely 1-butyl-3-methylimidazolium thiocyanate, $[C_4C_1im][SCN]$, 1-butyl-3-methylimidazolium dicyanamide, $[C_4C_1im][N(CN)_2]$, 1-butyl-3-methylimidazolium tricyanomethanide, $[C_4C_1im][C(CN)_3]$ that were acquired from IoLiTec (Germany) and 1-ethyl-3-methylimidazolium tetracyanoborate, $[C_2C_1im][B(CN)_4]$, from Merck KGaA Germany, all with mass fraction purities higher than 98%. The ILs chemical structures are shown in Table 1. To reduce both water and volatile compounds in the ILs to negligible values, vacuum (10^{-2} mbar), stirring, and moderate temperature (303 K) for a period of at least 48 h were applied prior to the measurements. ILs were also kept under vacuum (10^{-2} mbar) between uses. The final IL water content was determined with a Metrohm 831 Karl Fischer coulometer (using the Hydranal−Coulomat E from Riedel-de Haen as analyte), indicating a water mass fraction lower than 30×10^{-6} wt %. The purities of each IL were further checked by ^{1}H and ^{13}C NMR. The ethanol used was obtained from Merck with mass fraction purity higher than 99.8%. Being highly hygroscopic, the ethanol was kept with molecular sieves to ensure a low water content. The ethanol−water content measured was lower than 50×10^{-5} wt %. The water used was double distilled and deionized, passed through a reverse osmosis system and further treated with a Milli-Q plus 185 water purification equipment.

2.2. VLE Measurement. Apparatus and Procedures. VLE measurements were made with an isobaric micro-ebulliometer at different pressures: 0.05, 0.07, and 0.1 MPa. The apparatus used and the methodology adopted in this work have been previously optimized and are described in detail elsewhere.[15] The equilibrium temperature of the liquid phase was measured, with an uncertainty of 0.2 K, with a fast response glass-sealed Pt100 class 1/10, which was calibrated prior to the measurements by comparison with a NIST-certified Fluke RTD25 standard thermometer, with an uncertainty less than 2×10^{-2} K. The internal pressure of the ebulliometer was kept constant through a vacuum pump Buchi V-700 and a V-850 Buchi pressure monitoring and controller unit. The system pressure was monitored by a MKS, model 728A, Baratron type capacitance manometer, with temperature regulation at 100 °C to avoid solvent condensation and with an accuracy of 0.5%. Only when the equilibrium temperature was constant for 30 min or longer, the equilibrium conditions were assumed. The mixture composition was determined through an Anton Paar Abbemat 500 Refractometer, with an uncertainty of 2×10^{-5} nD, using a calibration curve previously established. The adequacy of the apparatus to measure this type of systems was previously confirmed.[15] Additionally, to test the apparatus, measurements of the VLE of pure compounds (ethanol, water, *p*-xylene, and decane) covering the temperature range of interest for the water + IL and ethanol + IL systems studied in this work were carried out. It was observed an uncertainty in the boiling temperatures of 0.2 K.

2.3. Density Measurement (Ethanol + IL Systems). In this work, mixtures of $[C_4C_1im][SCN]$, $[C_4C_1im][N(CN)_2]$, $[C_4C_1im][C(CN)_3]$, and $[C_2C_1im][B(CN)_4]$ with ethanol were prepared gravimetrically, with an uncertainty of $\pm 10^{-5}$ g, for subsequent measurement of density. In order to guarantee homogenization, mixtures were kept at constant stirring for 24 h, at room temperature in closed vials to minimize moisture absorption.

An automated SVM 3000 Anton Paar rotational Stabinger viscosimeter−densimeter was used to measure density data, at atmospheric pressure and at the temperature of 298.15 K. The viscosimeter−densimeter equipment uses Peltier elements for fast and efficient thermostatization, and has been widely used by us[40,48−50] for other systems composed of ILs. The uncertainty in temperature is within ±0.02 K and the absolute uncertainty for density is ±0.5 kg·m^{-3}. Obtained density data are compiled in Table S1 at the Supporting Information.

3. COMPUTATIONAL DETAILS

3.1. COSMO-RS. COSMO-RS combines the advantages and the computational efficiency of the quantum chemical dielectric continuum solvation model COSMO with a statistical thermodynamics approach, based on the results of the quantum chemical calculations.[51,52] The standard procedure of COSMO-RS calculations consists of two steps. First, the software TURBOMOLE 6.1 program package at the RI-DFT BP/TZVP level was used for the quantum-chemical calculation to generate the COSMO files for each studied compound. And second COSMO-RS calculations were performed in the COSMO-therm software using the parameter file BP_TZVP_C21_0110 (COSMOlogic GmbH & Co KG, Leverkusen, Germany).[51,52] Following the two-step procedure, COSMO-RS model has proved to be an excellent tool to evaluate qualitatively the strength of the interactions established by ILs with other compounds (binary or ternary systems), and consequently to predict their VLE,[32,35,53,54] activity coefficients,[55−58] liquid−liquid equilibria (LLE),[59−61] among other properties.[62] Therefore, COSMO-RS is going to be evaluated in the prediction of the experimental VLE data, and used to further understand the molecular level interactions as discussed below.

3.2. Molecular Dynamics Simulation. Molecular dynamics simulations were performed with the GROMACS[63] code, version 4.5.4, for the binary mixtures composed of ethanol and $[C_4C_1im][SCN]$, $[C_4C_1im][N(CN)_2]$, $[C_4C_1im][C(CN)_3]$, and $[C_2C_1im][B(CN)_4]$, at IL mole fractions of 0.2, 0.4, 0.6, and 0.8.

For all systems considered, after energy minimization and equilibration runs, production runs of 10 ns, within the canonical ensemble (*NVT*), were performed using a time step of 2 fs. The latter were followed by production runs of 20 ns, within the isothermal−isobaric (*NPT*) ensemble, at constant temperature of 298.15 K maintained using the Nosé−Hoover[64,65] thermostat, and at constant pressure of 1 bar maintained with the Parrinello−Rahman[66] barostat. The intermolecular interaction energy between pairs of neighboring atoms was calculated using the Lennard-Jones and the point-charge Coulomb potentials for describing dispersion/repulsion and electrostatic forces, respectively. Lennard-Jones and Coulombic interactions were defined setting the cutoffs to 1.2 and 1.0 nm, respectively, and long-range corrections for energy and pressure were also applied. Rigid constraints were enforced on all bonds lengths.

The force field parameters for the $[C_4C_1im]^+$ and $[C_2C_1im]^+$ cations, as well as for the $[SCN]^-$ anion were published in our previous work.[67] The potential parameters for the $[N(CN)_2]^-$ and $[C(CN)_3]^-$ anions were taken from the OPLS-AA force field,[68,69] and the $[B(CN)_4]^-$ anion were taken from the work

DOI: 10.1021/acs.jpcb.5b03324
J. Phys. Chem. B 2015, 119, 10287−10303

Table 2. Experimental Isobaric VLE Data for the System $[C_4C_1im][N(CN)_2]$ (1) + Water (2) at (0.1, 0.07, and 0.05) MPa Pressures[a]

0.1 MPa			0.07 MPa			0.05 MPa		
x_2	T/K	γ_2	x_2	T/K	γ_2	x_2	T/K	γ_2
1	372.89	0.997	1	363.22	0.996	1	354.66	0.995
0.998	373.07	0.994	0.999	363.35	0.992	0.999	354.80	0.990
0.997	373.08	0.994	0.999	363.59	0.981	0.997	354.63	0.999
0.983	373.52	0.993	0.996	363.70	0.982	0.995	354.71	0.998
0.975	373.84	0.992	0.988	363.87	0.984	0.987	354.87	1.000
0.966	374.16	0.988	0.972	364.08	0.992	0.971	355.31	0.991
0.955	374.45	0.990	0.963	364.25	0.995	0.953	354.97	1.013
0.948	374.75	0.988	0.954	364.55	0.991	0.981	355.71	0.989
0.944	374.84	0.986	0.947	364.77	0.993	0.928	355.14	1.025
0.937	375.17	0.982	0.943	364.90	0.991	0.949	355.78	1.003
0.933	375.22	0.984	0.940	364.94	0.994	0.932	356.33	1.001
0.931	375.24	0.984	0.935	365.02	0.994	0.965	356.19	1.007
0.921	375.83	0.973	0.929	365.22	0.995	0.915	356.58	1.007
0.907	376.28	0.978	0.924	365.52	0.989	0.911	357.24	0.987
0.906	376.43	0.971	0.908	366.31	0.976	0.894	357.30	1.002
0.890	377.16	0.967	0.890	366.92	0.975	0.886	357.92	0.987
0.879	377.61	0.959	0.880	367.36	0.970	0.855	358.26	0.994
0.864	378.41	0.951	0.858	368.45	0.955	0.868	358.04	1.018
0.852	379.25	0.935	0.849	368.79	0.953	0.840	359.46	0.982
0.832	380.41	0.923	0.823	369.98	0.941	0.828	360.39	0.961
0.816	381.52	0.908	0.805	370.69	0.938	0.809	361.29	0.951
0.807	382.04	0.901	0.792	372.19	0.904	0.796	362.39	0.928
0.786	383.73	0.874	0.781	372.39	0.909	0.783	362.87	0.923
0.761	385.60	0.845	0.758	374.41	0.872	0.756	364.39	0.906
0.758	385.82	0.845	0.751	375.20	0.856	0.751	365.22	0.880
0.716	389.97	0.782	0.725	377.63	0.814	0.717	367.28	0.859
0.717	389.99	0.782	0.704	379.30	0.792	0.705	368.53	0.830
0.683	392.96	0.744	0.681	380.94	0.774	0.681	370.26	0.804
0.679	393.11	0.746	0.677	381.08	0.776	0.678	370.75	0.796
0.661	394.88	0.724	0.656	382.75	0.756	0.670	371.28	0.795
0.645	396.41	0.707	0.641	384.27	0.735	0.648	373.12	0.764
0.631	398.25	0.683	0.625	386.05	0.711	0.632	374.91	0.737
0.612	400.16	0.664	0.610	388.19	0.679	0.617	376.41	0.715
0.586	403.87	0.621	0.566	392.26	0.641	0.575	379.34	0.693
0.562	406.78	0.593	0.561	392.82	0.635	0.567	380.54	0.675
0.545	408.85	0.576	0.527	396.16	0.609	0.531	383.99	0.642
0.509	416.61	0.496	0.494	400.88	0.562	0.494	389.87	0.568
0.473	425.31	0.422	0.462	404.36	0.542	0.462	393.60	0.538

[a]Standard uncertainties x, T, and γ are 0.001, 0.2 K, and 0.001, respectively.

of Koller et al.[70] The atomic charges for the IL cations and anions were recalculated with the CHelpG scheme[71] using an optimized geometry (minimum energy among different configurations), for each IL ion pair, in the gaseous phase as performed previously for other systems involving ILs.[39,67] The calculations were performed at the B3LYP/6-311+G(d) level of theory[72] using the Gaussian 09 code.[73] The total charges on the cations and anions were ±0.804 e for $[C_4C_1im][SCN]$, ± 0.826 e for $[C_4C_1im][N(CN)_2]$, ± 0.882 e for $[C_4C_1im][C(CN)_3]$ and ±0.889 e for $[C_2C_1im][B(CN)_4]$. The full sets of atomic charges for each IL were reported elsewhere.[74] The parameters for ethanol were also taken from the OPLS-AA force field.[68,69]

For validation of the applied force field, density and enthalpy of vaporization were calculated. The latter was obtained according to eq 1,

$$\Delta H^{vap} = RT - (U^{liq} - U^{vap}) \quad (1)$$

where ΔH^{vap} is the enthalpy of vaporization, R is the ideal gas constant, T is the temperature, and U^{vap} and U^{liq} are the molar internal energies of the gaseous and of the liquid phases, respectively. To reproduce the gas phase, isolated IL ion pairs were considered and simulations were performed at the same temperature of the liquid phase.

In addition, radial and spatial distributions functions and coordination numbers were also calculated from the MD trajectories of all mixtures considered.

4. RESULTS AND DISCUSSIONS

4.1. VLE Measurements and COSMO-RS Predictions.

Isobaric VLE data of the binary systems $[C_4C_1im][SCN]$, $[C_4C_1im][N(CN)_2]$, $[C_4C_1im][C(CN)_3]$ and $[C_2C_1im][B(CN)_4]$ with water and ethanol were measured at 0.1, 0.07, and 0.05 MPa, and are reported in Table 2 to 8 and depicted in Figure 1 and 2 along with the COSMO-RS predictions. The experimental boiling temperature is represented as a function of

DOI: 10.1021/acs.jpcb.5b03324
J. Phys. Chem. B 2015, 119, 10287−10303

Table 3. Experimental Isobaric VLE Data for the System $[C_4C_1im][C(CN)_3]$ (1) + Water (2) at (0.1, 0.07, and 0.05) MPa Pressures[a]

0.1 MPa			0.07 MPa			0.05 MPa		
x_2	T/K	γ_2	x_2	T/K	γ_2	x_2	T/K	γ_2
1	372.89	0.997	1	363.22	0.996	1	354.66	0.995
0.828	376.55	1.059	0.817	366.62	1.071	0.825	357.52	1.077
0.780	378.38	1.055	0.778	368.06	1.067	0.809	357.93	1.085
0.739	380.85	1.024	0.741	369.83	1.051	0.740	360.37	1.072
0.720	381.98	1.011	0.728	370.35	1.050	0.727	361.25	1.054
0.703	382.84	1.006	0.708	371.23	1.045	0.714	361.56	1.061
0.690	383.65	0.994	0.683	372.39	1.039	0.696	362.29	1.060
0.663	385.21	0.984	0.672	373.37	1.021	0.675	362.99	1.063
0.643	386.56	0.971	0.656	374.14	1.017	0.663	363.63	1.056
0.620	387.86	0.963	0.645	374.9	1.005	0.648	364.41	1.053
0.606	389.35	0.939	0.616	377.22	0.972	0.630	365.69	1.030
0.595	390.39	0.925	0.582	379.35	0.955	0.613	366.80	1.014
0.581	391.73	0.911	0.553	381.30	0.942	0.597	367.81	1.005
0.557	393.62	0.893	0.539	382.62	0.924	0.564	370.30	0.970
0.552	394.48	0.877	0.530	383.35	0.917	0.548	372.14	0.934
0.532	396.25	0.861	0.526	384.16	0.900	0.489	376.27	0.905
0.500	399.35	0.833	0.494	386.63	0.881	0.473	377.39	0.900
0.481	401.16	0.819	0.484	387.43	0.877	0.450	379.15	0.889
0.465	402.97	0.802	0.481	387.55	0.879	0.442	380.15	0.876
0.438	405.71	0.785	0.482	387.99	0.865	0.433	381.19	0.862
0.421	408.27	0.759	0.450	390.1	0.865	0.419	382.68	0.847
0.406	410.22	0.744	0.425	393.07	0.832	0.419	383.07	0.836
0.389	412.43	0.728	0.418	394.13	0.819	0.439	380.66	0.867
0.385	413.66	0.711	0.412	395.17	0.803	0.404	385.82	0.792
0.374	414.83	0.707	0.376	400.51	0.748	0.444	380.15	0.871
0.370	415.15	0.709	0.370	402.15	0.722	0.421	382.15	0.860

[a]Standard uncertainties x, T, and γ are 0.001, 0.2 K and 0.001, respectively.

Table 4. Experimental Isobaric VLE Data for the System $[C_2C_1im][B(CN)_4]$ (1) + Water (2) at (0.1, 0.07, and 0.05) MPa Pressures[a]

0.1 MPa			0.07 MPa			0.05 MPa		
x_2	T/K	γ_2	x_2	T/K	γ_2	x_2	T/K	γ_2
1	372.89	0.997	1	363.22	0.996	1	354.66	0.995
0.237	419.61	0.975	0.277	404.15	0.910	0.237	395.15	1.001
0.313	408.07	1.023	0.334	392.21	1.092	0.289	385.60	1.117
0.353	402.87	1.057	0.368	387.66	1.147	0.320	380.38	1.201
0.376	400.36	1.072	0.376	385.42	1.208	0.333	378.36	1.238
0.391	397.97	1.108	0.396	383.26	1.233	0.346	376.16	1.284
0.408	395.15	1.159	0.412	381.98	1.238	0.380	371.55	1.380
0.423	392.87	1.201	0.427	378.58	1.341	0.407	368.55	1.437
0.445	390.55	1.230	0.440	378.06	1.325	0.435	365.29	1.515
0.452	389.26	1.264	0.465	374.93	1.398	0.460	361.55	1.653
0.465	388.17	1.273	0.475	374.03	1.413	0.494	359.46	1.668
0.483	386.18	1.310	0.485	372.36	1.469	0.520	357.29	1.723
0.509	384.71	1.304	0.524	369.86	1.486	0.542	356.46	1.710
0.535	382.40	1.341	0.558	367.18	1.540	0.558	355.63	1.717
0.580	380.17	1.334	0.588	365.27	1.570	0.606	354.87	1.628
0.601	379.23	1.329	0.595	364.82	1.579	0.627	354.47	1.601
0.620	378.38	1.326	0.601	364.58	1.577	0.645	354.18	1.573

[a]Standard uncertainties x, T, and γ are 0.001, 0.2 K, and 0.001, respectively.

the mole fraction of water/ethanol and compared with the COSMO-RS predictions, in the region of complete miscibility. The COSMO-RS model prediction for the binary system $[C_4C_1im][SCN]$, $[C_4C_1im][N(CN)_2]$, $[C_4C_1im][C(CN)_3]$, and $[C_2C_1im][B(CN)_4]$ with water and ethanol is found to be in close agreement with the experimental boiling points for mole fractions higher than 0.8. Afterward, the quality of the predictions degrades with the ILs concentration, for which only a qualitative prediction is achieved, as observed in previous works.[55,75]

For the studied systems, and to the best of our knowledge, the VLE data is here reported for the first time. Orchilles et al.[25]

DOI: 10.1021/acs.jpcb.5b03324
J. Phys. Chem. B 2015, 119, 10287−10303

Table 5. Experimental Isobaric VLE Data for the System $[C_4C_1im][SCN]$ (1) + Ethanol (2) at (0.1, 0.07, and 0.05) MPa Pressures[a]

0.1 MPa			0.07 MPa			0.05 MPa		
x_2	T/K	γ_2	x_2	T/K	γ_2	x_2	T/K	γ_2
1	351.15	0.999	1	342.36	0.999	1	334.63	0.996
0.982	351.49	0.996	0.981	342.71	1.006	0.982	334.98	0.996
0.981	351.58	0.994	0.979	342.93	0.997	0.973	335.16	1.000
0.963	351.98	0.997	0.963	343.24	1.001	0.961	335.60	0.993
0.943	352.07	1.014	0.943	343.65	1.004	0.933	336.36	0.989
0.921	352.54	1.019	0.919	344.15	1.009	0.914	336.84	0.989
0.892	353.60	1.015	0.897	344.82	1.007	0.895	337.33	0.989
0.870	354.38	1.010	0.850	346.60	0.988	0.871	338.27	0.976
0.834	355.61	1.005	0.832	347.44	0.975	0.840	339.41	0.963
0.794	357.46	0.984	0.807	348.72	0.954	0.795	341.42	0.934
0.781	358.17	0.968	0.790	349.53	0.945	0.775	342.53	0.914
0.767	358.97	0.956	0.770	350.44	0.934	0.759	343.40	0.901
0.693	362.96	0.911	0.690	355.06	0.870	0.698	346.71	0.855
0.675	363.98	0.898	0.681	355.50	0.867	0.681	347.91	0.835
0.628	366.62	0.878	0.623	358.82	0.836	0.628	350.64	0.811
0.593	368.91	0.867	0.584	360.90	0.825	0.595	352.53	0.795
0.570	370.73	0.846	0.572	362.18	0.804	0.570	354.33	0.774
0.531	373.01	0.841	0.523	365.63	0.775	0.530	356.71	0.759
0.501	374.93	0.836	0.416	372.71	0.760	0.490	359.18	0.749
0.407	382.38	0.806	0.399	375.08	0.732	0.424	364.45	0.714
0.344	388.81	0.778	0.350	379.50	0.720	0.360	370.15	0.687
0.313	392.38	0.766	0.315	383.06	0.712	0.333	372.45	0.684
0.241	402.38	0.740	0.243	391.97	0.700	0.282	377.45	0.680

[a]Standard uncertainties x, T, and γ are 0.001, 0.2 K, and 0.001, respectively.

reported VLE data for the binary mixture for $[C_2C_1im][N(CN)_2]$ with water and ethanol that, in comparison with that of $[C_4C_1im][N(CN)_2]$, denotes the well-established weak cation influence on the systems boiling temperatures, within the range of mole fraction investigated, as depicted in the Supporting Information (Figure S1). The isobaric VLE data for $[C_4C_1im][SCN]$ + water at 0.1, 0.07, and 0.05 MPa was adapted from Passos et al.,[18] Figure 1 and 2 report the VLE of the studied systems as a function of composition, temperature and pressure. It can be seen that pressure does not have a strong influence on the shape of the boiling-point elevation dependency with the concentration, as shown by the parallel behavior of the temperature−composition equilibrium curves at the different pressures (for variation of activity coefficient see Supporting Information, Figure S2).

The measured boiling temperatures decrease with increasing solvent concentration as expected and shown in Figures 1, 2, and 3, and the influence of ILs on the boiling temperature of both water and ethanol seems to follow the trend, $[C_4C_1im][N(CN)_2]$ > $[C_4C_1im][SCN]$ > $[C_4C_1im][C(CN)_3]$ > $[C_2C_1im][B(CN)_4]$, which is identical to the trend of mutual solubility of water and $[C_4C_1pyr]^+$-based ILs reported by Królikowska et al.[76]

It is well established that the anion plays a primordial role in the IL interaction with water.[77−79] Regarding the studied ILs, the imidazolium cation was fixed with the aim of studying the differentiation between the anions interactions with water and ethanol. The hydrogen bonding capability of the cyano group with water/ethanol was expected to increase with the number of cyano groups in the anion. However, although the expected increase on the number of interaction positions is observed for $[C_4C_1im][SCN]$ and $[C_4C_1im][N(CN)_2]$, the reversed behavior with further increase of the number of cyano groups is perceived for the other two compounds in the anion series $[C(CN)_3]^-$ and $[B(CN)_4]^-$. As shown in recent work,[74] using COSMO-RS (sigma profile and potential), the high polarity of the anion $[N(CN)_2]^-$ leads to a higher capability to establish hydrogen bonds (H-bond donors) than $[SCN]^-$. In that work it was found also that by increasing the number of cyano groups from $[N(CN)_2]^-$ to $[C(CN)_3]^-$ and to $[B(CN)_4]^-$, the ability of these anions to act as H-bond acceptors decrease. As a consequence, it is expected that $[N(CN)_2]^-$ presents stronger interactions with water/ethanol than $[SCN]^-$, $[C(CN)_3]^-$ and $[B(CN)_4]^-$ besides the lower number of the interaction position/groups could be interpreted as a consequence of the change in their charge distribution due to the partial geometric dipole moment cancelation.

4.1.1. Activity Coefficients. The effect of an IL on the nonideality of a solution can be expressed by the activity coefficient of component i, γ_i, which can be estimated from the vapor liquid equilibrium data by the equation

$$\gamma_i = y_i\phi_i p / x_i\phi_i^s p_i^s \quad (2)$$

where p and p_i^S are the pressure of the system and the saturation pressure of the pure component i at the system temperature, y_i and x_i represent the mole fractions of component i in the vapor and liquid phases, respectively, ϕ_i is the fugacity coefficient of component i in the vapor phase, while ϕ_i^S is the fugacity coefficient of component i in its saturated state. The fugacity coefficients ϕ_i and ϕ_i^S are close to unity at the pressures used in this study, and since the IL is nonvolatile, the vapor phase is only composed of solvent which leads to y_i equal to unity. Thus, the activity coefficient of solvent in solution can be simplified as

$$\gamma_i = p / x_i p_i^s \quad (3)$$

DOI: 10.1021/acs.jpcb.5b03324
J. Phys. Chem. B 2015, 119, 10287−10303

Table 6. Experimental Isobaric VLE Data for the System $[C_4C_1im][N(CN)_2]$ (1) + Ethanol (2) at (0.1, 0.07, and 0.05) MPa Pressures[a]

0.1 MPa			0.07 MPa			0.05 MPa		
x_2	T/K	γ_2	x_2	T/K	γ_2	x_2	T/K	γ_2
1	351.15	0.999	1	342.36	0.999	1	334.63	0.996
0.984	351.55	1.000	0.984	342.81	0.998	0.985	334.88	1.000
0.948	352.61	0.998	0.954	343.47	1.001	0.963	335.67	0.988
0.940	352.80	0.999	0.946	343.53	1.007	0.954	335.81	0.991
0.904	353.92	0.994	0.921	344.69	0.985	0.920	336.87	0.981
0.875	355.64	0.960	0.893	345.68	0.974	0.902	337.36	0.980
0.865	355.96	0.961	0.889	346.08	0.964	0.887	337.97	0.970
0.860	356.22	0.956	0.879	346.42	0.962	0.852	339.10	0.962
0.843	356.91	0.948	0.861	347.24	0.949	0.834	340.31	0.933
0.813	358.15	0.940	0.832	349.06	0.913	0.823	340.70	0.931
0.801	359.01	0.925	0.821	349.34	0.915	0.831	340.56	0.927
0.783	359.94	0.912	0.806	350.07	0.905	0.790	342.26	0.908
0.760	361.03	0.903	0.790	350.94	0.893	0.789	342.38	0.904
0.751	361.43	0.899	0.786	351.17	0.889	0.738	345.65	0.844
0.742	361.93	0.895	0.774	351.54	0.890	0.734	345.69	0.848
0.716	363.38	0.879	0.730	354.20	0.850	0.725	346.73	0.822
0.695	364.51	0.870	0.719	354.97	0.838	0.710	347.79	0.806
0.656	366.86	0.849	0.695	356.31	0.825	0.675	349.31	0.796
0.634	368.27	0.834	0.674	357.28	0.819	0.641	351.19	0.778
0.610	369.74	0.823	0.637	359.69	0.792	0.637	351.49	0.774
0.601	370.27	0.819	0.633	360.12	0.783	0.626	352.15	0.769
0.596	370.49	0.821	0.616	361.21	0.775	0.613	352.91	0.761
0.585	371.49	0.806	0.604	361.96	0.767	0.613	353.10	0.755
0.540	375.00	0.777	0.593	362.64	0.763	0.569	356.02	0.726
0.531	375.84	0.768	0.575	363.91	0.751	0.559	356.71	0.721
0.500	377.84	0.762	0.523	367.12	0.735	0.536	358.02	0.716
0.486	378.88	0.757	0.498	369.42	0.713	0.491	360.51	0.711
0.466	380.54	0.748	0.490	370.04	0.708	0.465	362.56	0.696
0.448	382.48	0.732	0.464	372.03	0.698	0.465	362.82	0.690
0.441	383.26	0.725	0.452	373.36	0.685	0.448	363.99	0.686
0.427	384.42	0.721	0.426	375.66	0.672	0.434	365.43	0.673
0.403	387.55	0.692	0.403	378.38	0.650	0.414	368.09	0.643
0.386	389.47	0.679	0.371	381.51	0.635	0.377	372.43	0.605
0.363	392.44	0.661	0.369	381.66	0.637	0.370	372.80	0.609
0.354	393.74	0.651	0.357	383.24	0.626	0.369	373.39	0.598
0.342	395.38	0.642	0.337	385.43	0.618	0.338	377.27	0.573
0.340	395.56	0.643	0.319	387.72	0.608	0.330	379.34	0.549
0.313	399.26	0.626	0.299	390.54	0.592	0.308	382.19	0.536
0.306	400.51	0.616	0.286	392.96	0.577	0.305	383.14	0.525
0.293	403.72	0.589	0.278	394.74	0.563	0.300	384.79	0.507
0.285	406.86	0.553	0.262	397.08	0.557	0.294	385.45	0.505

[a]Standard uncertainties x, T, and γ are 0.001, 0.2 K, and 0.001, respectively.

where subscript i refers to solvents such as water or ethanol. The pure component saturation pressure p_i^S, of water and ethanol were estimated using correlations obtained from DIPPR's database.[80]

The activity coefficients estimated for the studied systems are reported in Table 2 to 8 and depicted in Figure 4 at 0.1 MPa along with the COSMO-RS predictions (for other system pressures, see Figure S2 of the Supporting Information). As depicted in Figure 3, the activity coefficients evidence the behavior observed for the systems boiling temperatures, with the activity coefficients decreasing from the [SCN] to $[N(CN)_2]$ but increasing afterward for the $[C(CN)_3]$ and $[B(CN)_4]$. As discussed above, the high polarity of the anion $[N(CN)_2]^-$ [74] leads to a higher capability to establish hydrogen bonds (H-bond donors) leading therefore, to the lowest activity coefficients of the series. Furthermore, as shown previously,[74] the increase in the number of cyano groups in the series $[N(CN)_2]^-$, $[C(CN)_3]^-$ and $[B(CN)_4]^-$ leads to a decrease on the ability of these anions to act as H-bond acceptors and therefore to an increase of the compounds' activity coefficients, as depicted in Figure 3.

For the ethanol-containing mixtures the activity coefficient data suggest that the interactions are weaker than those present in aqueous systems with the deviation to ideality following the trend $[C_4C_1im][N(CN)_2] < [C_4C_1im][SCN] < [C_4C_1im][C(CN)_3] < [C_2C_1im][B(CN)_4]$. The differences between $[C_4C_1im][N(CN)_2]$ and $[C_4C_1im][SCN]$, as well as between $[C_4C_1im][C(CN)_3]$ and $[C_2C_1im][B(CN)_4]$, are, however, less pronounced than those in aqueous systems where the hydrogen bonding is more intense.

DOI: 10.1021/acs.jpcb.5b03324
J. Phys. Chem. B 2015, 119, 10287−10303

Table 7. Experimental Isobaric VLE Data for the System $[C_4C_1im][C(CN)_3]$ (1) + Ethanol (2) at (0.1, 0.07, and 0.05) MPa Pressures[a]

0.1 MPa			0.07 MPa			0.05 MPa		
x_2	T/K	γ_2	x_2	T/K	γ_2	x_2	T/K	γ_2
1	351.15	0.999	1	342.36	0.999	1	334.63	0.996
0.999	351.20	0.999	0.996	342.50	0.996	0.991	334.65	1.008
0.996	351.35	0.996	0.991	342.55	1.002	0.967	334.95	1.017
0.968	351.65	1.012	0.962	342.95	1.013	0.960	335.15	1.013
0.963	351.81	1.014	0.948	343.25	1.015	0.948	335.53	1.014
0.947	352.00	1.024	0.948	343.29	1.018	0.937	335.55	1.025
0.948	352.12	1.016	0.937	343.45	1.022	0.941	335.63	1.012
0.937	352.27	1.022	0.930	343.47	1.024	0.927	335.85	1.018
0.920	352.60	1.026	0.920	343.75	1.026	0.920	336.04	1.024
0.929	352.34	1.027	0.909	344.05	1.024	0.907	336.18	1.026
0.909	353.01	1.022	0.909	344.24	1.019	0.908	336.35	1.019
0.909	352.89	1.029	0.892	344.60	1.023	0.889	336.82	1.022
0.890	353.38	1.027	0.881	344.86	1.021	0.879	337.18	1.015
0.878	353.92	1.022	0.868	345.29	1.019	0.868	337.51	1.007
0.865	354.06	1.030	0.860	345.54	1.017	0.854	337.92	1.010
0.856	354.70	1.017	0.838	346.48	1.007	0.838	338.61	1.001
0.834	355.36	1.018	0.828	346.67	1.009	0.828	338.59	1.014
0.828	355.59	1.017	0.808	347.79	0.987	0.805	339.45	1.005
0.804	356.59	1.009	0.795	348.13	0.994	0.795	339.55	1.013
0.796	356.79	1.010	0.786	348.40	0.992	0.786	340.22	0.990
0.787	357.19	1.005	0.784	348.77	0.978	0.784	340.43	0.990
0.788	357.29	1.002	0.768	349.65	0.963	0.768	341.25	0.976
0.773	357.94	0.997	0.754	349.68	0.967	0.753	341.50	0.987
0.754	358.74	0.990	0.735	350.47	0.978	0.757	342.12	0.952
0.753	358.81	0.987	0.749	350.64	0.950	0.735	342.29	0.978
0.735	359.71	0.979	0.735	351.29	0.943	0.734	342.96	0.948
0.738	359.82	0.970	0.725	351.88	0.935	0.717	343.69	0.942
0.712	360.89	0.968	0.711	352.50	0.935	0.711	343.72	0.951
0.720	361.04	0.951	0.706	352.86	0.923	0.699	344.54	0.933
0.701	362.23	0.935	0.675	354.80	0.896	0.671	345.58	0.933
0.671	363.24	0.941	0.670	354.96	0.901	0.674	345.95	0.914
0.671	363.95	0.917	0.645	356.55	0.881	0.644	347.13	0.911
0.649	365.59	0.895	0.618	357.95	0.870	0.618	348.49	0.899
0.627	366.79	0.889	0.589	359.56	0.859	0.590	349.75	0.895
0.603	368.55	0.866	0.559	361.71	0.834	0.560	351.73	0.872
0.572	370.39	0.852	0.539	363.11	0.822	0.539	353.27	0.852
0.562	371.15	0.845	0.507	365.32	0.807	0.521	354.05	0.856
0.538	372.90	0.830						

[a]Standard uncertainties x, T, and γ are 0.001, 0.2 K, and 0.001, respectively.

4.2. MD Simulations. *4.2.1. Validation of MD Simulations.* To complement the experimental part of this study, MD simulations were performed for the systems containing the CN-based ILs and ethanol. For the aqueous systems containing the same ILs, MD simulations were already performed and discussed in a previous study.[74]

Density estimation is usually used to recognize the ability of a force field to reproduce a system.[81] As mentioned in the computational detail section, pure ILs force fields were tested and accordingly to density estimation, they were considered to be able to reproduce the behavior of these pure ILs. In Table S2 of the Supporting Information are compiled values of experimental and simulated densities and enthalpies of vaporization for pure ILs. A good agreement is obtained for density values, but for the values of enthalpies, as expected, differences can reach tens of kJ/mol, associated with the lack of accuracy and difficulty of measuring experimentally this property.[39]

Furthermore, and using the density data measured in this study for mixtures of CN-based ILs and ethanol, a comparison between experimental data and density values obtained from our simulations was also made, as compiled in **Table S1** of Supporting Information. The maximum deviation obtained was in the order of 3%, suggesting that the force fields adopted provide also a good structural description of the mixtures with ethanol.

4.2.2. Radial distribution function and coordination numbers. Radial distribution function, $g(r)$ or RDF, and coordination numbers (Z) are commonly used in MD simulations to evaluate and describe the atomic local structural organization of mixtures. The first gives the probability of finding a particle at the distance r, from another particle (considered the reference), providing a quantitative description of enhancement or depletion of densities of atoms, or groups of atoms, around a selected moiety with respect to bulk values. The second, the coordination number, is the average number of

DOI: 10.1021/acs.jpcb.5b03324
J. Phys. Chem. B 2015, 119, 10287−10303

Table 8. Experimental Isobaric VLE Data for the System $[C_2C_1im][B(CN)_4]$ (1) + Ethanol (2) at (0.1, 0.07, and 0.05) MPa Pressures[a]

0.1 MPa			0.07 MPa			0.05 MPa		
x_2	T/K	γ_2	x_2	T/K	γ_2	x_2	T/K	γ_2
1	351.15	0.999	1	342.36	0.9995	1	334.63	0.996
0.983	351.21	1.016	0.994	342.50	1.001	0.993	334.64	1.000
0.969	351.27	1.025	0.972	342.59	1.020	0.973	334.76	1.016
0.994	351.32	0.998	0.983	342.68	1.005	0.983	334.83	1.004
0.986	351.34	1.004	0.963	342.73	1.023	0.970	334.88	1.013
0.976	351.43	1.011	0.970	342.83	1.009	0.963	334.94	1.014
0.952	351.52	1.034	0.943	342.93	1.036	0.943	335.16	1.029
0.964	351.55	1.018	0.957	342.96	1.019	0.952	335.20	1.022
0.949	351.66	1.029	0.921	343.17	1.051	0.932	335.49	1.032
0.933	351.79	1.043	0.933	343.36	1.029	0.918	335.61	1.042
0.936	351.80	1.041	0.899	343.50	1.062	0.920	335.66	1.038
0.917	351.89	1.053	0.918	343.54	1.036	0.900	335.70	1.053
0.910	352.00	1.056	0.892	343.73	1.060	0.898	335.87	1.052
0.918	352.14	1.046	0.884	343.97	1.059	0.889	335.90	1.055
0.902	352.22	1.057	0.899	344.01	1.040	0.877	336.14	1.058
0.897	352.55	1.057	0.868	344.29	1.064	0.878	336.20	1.059
0.886	352.67	1.057	0.878	344.41	1.047	0.851	336.74	1.060
0.879	352.84	1.059	0.859	344.65	1.059	0.854	336.94	1.049
0.878	352.96	1.060	0.866	344.69	1.051	0.847	336.98	1.059
0.866	353.22	1.065	0.854	344.86	1.056	0.842	337.10	1.060
0.863	353.31	1.058	0.849	344.88	1.062	0.836	337.25	1.059
0.854	353.50	1.066	0.839	345.29	1.058	0.834	337.27	1.057
0.851	353.73	1.062	0.833	345.43	1.054	0.831	337.46	1.059
0.834	354.03	1.070	0.822	345.74	1.061	0.815	337.89	1.062
0.838	354.15	1.061	0.807	346.16	1.061	0.807	337.90	1.067
0.816	354.70	1.066	0.801	346.39	1.063	0.779	338.70	1.063
0.808	354.83	1.072	0.774	347.10	1.062	0.775	339.05	1.065
0.791	355.42	1.069	0.770	347.25	1.066	0.769	339.07	1.063
0.773	356.02	1.069	0.754	347.80	1.066	0.759	339.47	1.061
0.780	356.03	1.060	0.742	348.29	1.061	0.723	340.60	1.063
0.767	356.49	1.059	0.719	349.17	1.049	0.716	340.80	1.062
0.739	357.43	1.060	0.706	349.51	1.062	0.722	340.94	1.053
0.722	358.25	1.052	0.704	349.69	1.056	0.710	341.19	1.059
0.718	358.29	1.057	0.701	349.73	1.057	0.699	341.60	1.057
0.695	359.12	1.058	0.696	349.91	1.058	0.701	341.73	1.049
0.672	360.33	1.046	0.686	350.51	1.049	0.682	341.99	1.059
0.658	361.12	1.037	0.673	350.96	1.052	0.657	343.61	1.035
0.623	362.33	1.042	0.657	351.79	1.039	0.645	343.84	1.042
0.607	363.75	1.022	0.645	352.29	1.035	0.630	344.73	1.030
0.599	363.89	1.030	0.639	352.61	1.034	0.612	345.84	1.013
0.580	364.82	1.028	0.619	353.84	1.018	0.607	346.35	1.002
0.582	365.09	1.015	0.606	354.63	1.008	0.579	347.40	0.992
0.562	366.18	1.012	0.589	355.60	1.002	0.575	347.86	0.989
0.562	366.36	1.005	0.575	356.57	0.988	0.562	348.67	0.981
0.547	366.99	1.011	0.573	356.93	0.977	0.547	349.56	0.971
0.548	367.20	0.999	0.562	357.58	0.974	0.542	349.77	0.965
0.527	368.44	0.991	0.560	357.83	0.965			

[a]Standard uncertainties x, T, and γ are 0.001, 0.2 K, and 0.001, respectively.

atoms of one type surrounding the reference atom within a cutoff, r_Z, given by the integral of RDF. The cutoff is usually chosen to be the first local minimum of the corresponding RDF. Figure 5 and S3 in the SI, provide all the RDFs for the mixtures considered, and Table 9 compiled the Z numbers estimated for all mixtures and type of interactions.

The analysis of the anion−solvent, cation−solvent, cation−anion, and solvent−solvent interactions were based on the site-to-site RDFs obtained for the N−HO, H1−OH, H1−N, and OH−HO pairs, respectively, where N is the nitrogen atom of each anion, H1 is the acidic proton of the cation, and HO and OH stand for protons and oxygen atoms in the ethanol molecule, respectively.

The first important feature that can be highlighted is the possibility to verify through the obtained RDFs the profile of these interactions, namely the establishment of hydrogen bonds similar to the ones occurring in aqueous systems.[74] The stronger H-bonds are recognizable by the presence of a site-to-

DOI: 10.1021/acs.jpcb.5b03324
J. Phys. Chem. B 2015, 119, 10287−10303

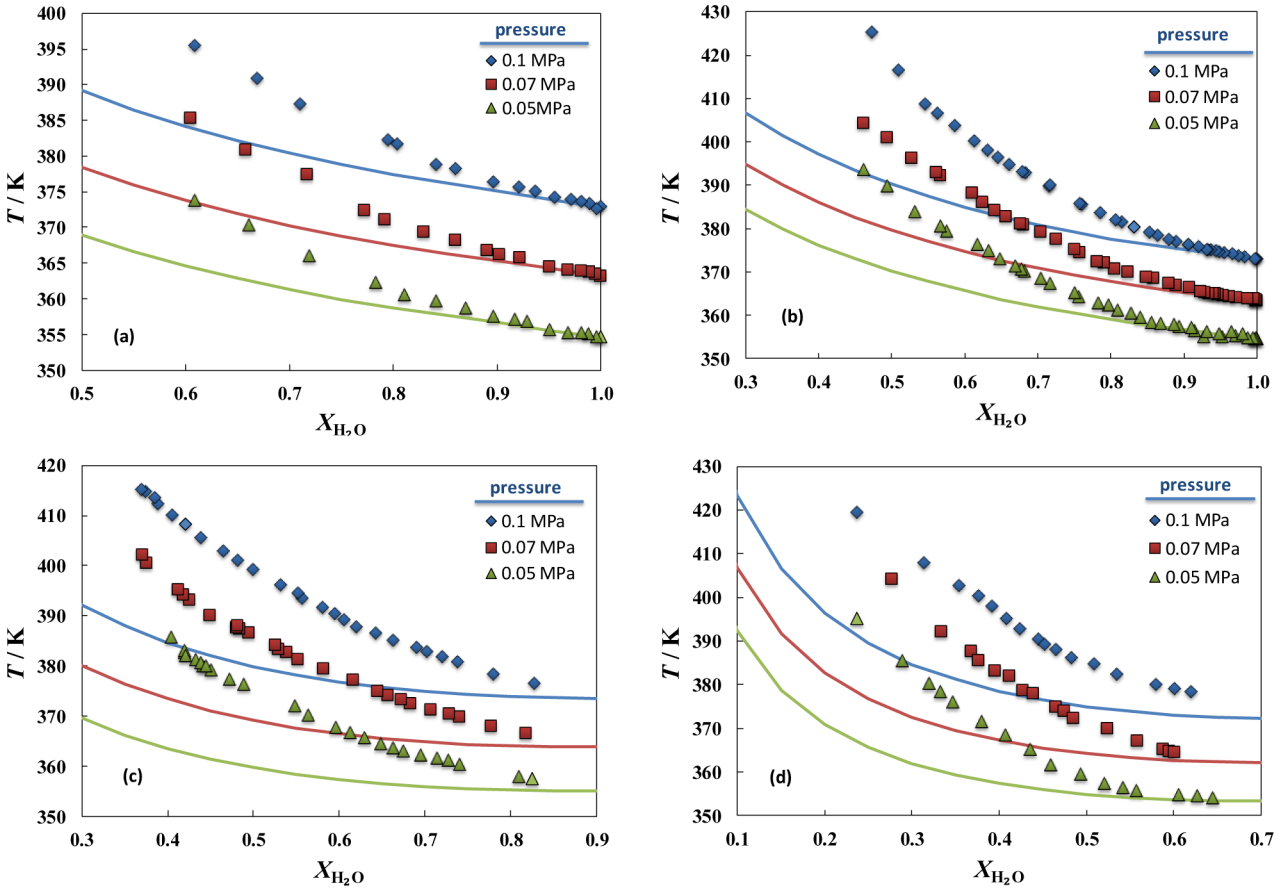

Figure 1. Isobaric temperature−composition diagram of (a) $[C_4C_1im][SCN]$ + water,[18] (b) $[C_4C_1im][N(CN)_2]$ + water, (c) $[C_4C_1im][C(CN)_3]$ + water, and (d) $[C_2C_1im][B(CN)_4]$ + water. The solid lines represent COSMO-RS predictions.

site RDF Y−H−X with a first minimum (r_z) in a distance smaller than 0.26 nm, where Y is an oxygen or nitrogen atom and X an oxygen atom, or weaker H-bonds, presenting a site-to-site RDF with the first minimum in a distance smaller than 0.40 nm, where Y is an oxygen or nitrogen atom and X a carbon atom.[82] In the studied systems, the first minimum found was 0.26 and 0.35 nm for anion-solvent and solvent−solvent interactions, and cation-solvent and cation−anion interactions, respectively. As mentioned previously, this first minimum is used to estimate the coordination numbers, which are compiled in Table 9.

Additionally, Figure 5 shows that the anion-solvent interaction has a primary role in the interaction occurring between IL and ethanol, which was expected to be common for all CN-based ILs (also observed for aqueous systems), presenting the highest values for the system containing the anion thiocyanate, followed by $[N(CN)_2]^-$, $[C(CN)_3]^-$ and finally $[B(CN)_4]^-$. Ensuing the anion-solvent interaction and in the same solvation shell, the solvent−solvent interactions occur, being predominant in systems containing the anion $[B(CN)_4]^-$. It is worth noting that solvent−solvent interactions depict a double peak of RDF, suggesting the formation of ethanol clustering in all IL + ethanol systems. In general, the double peak is more pronounced in the system with the anion tetracyanoborate, followed by $[C(CN)_3]^-$ > $[SCN]^-$ > $[N(CN)_2]^-$. This last trend is also observed for the cation−anion interactions occurring at the second solvation shell. Both these latter interactions present the trend that is consistent with the VLE measurements and nonideality as estimated from the activity coefficients. Simultaneously, at contrary to what has been observed for aqueous systems[74] and the values of $g(r)$ corresponding to the interactions established between cation and the solvent suggest that in the case of IL + ethanol systems they are non-negligible.

A more exhaustive comparison between the different systems is possible by the analysis of the coordination numbers, Z, since their values are obtained by taking into account not only the heights of the first peaks in the RDFs, but also their widths and the densities of the different systems. Thus, the values of Z help to clarify the interaction trend within the CN-based ILs and ethanol, providing important additional information concerning the nature of the interaction between compounds.

Table 9 compiles the calculated coordination numbers for the interactions anion-solvent, cation-solvent, cation−anion, solvent−solvent and finally, IL-solvent. The latter interaction is the sum of the cation-ethanol and anion-ethanol interactions in all range of concentration, enabling to infer general trends of all involved interactions. The first information that can be taken is the dependence of Z with the mole fraction of IL. Results show that, with the exception of cation−anion interactions, with the increase of IL's mole fraction the interaction of type anion-solvent, cation-solvent and solvent−solvent decrease, as shown by a decrease of the respective Z values. Although these results are a consequence of different densities in each system, they suggest that, with the increase of IL's mole fraction, the frequency of cation−anion interactions also increase, hindering the interaction with ethanol.

DOI: 10.1021/acs.jpcb.5b03324
J. Phys. Chem. B 2015, 119, 10287−10303

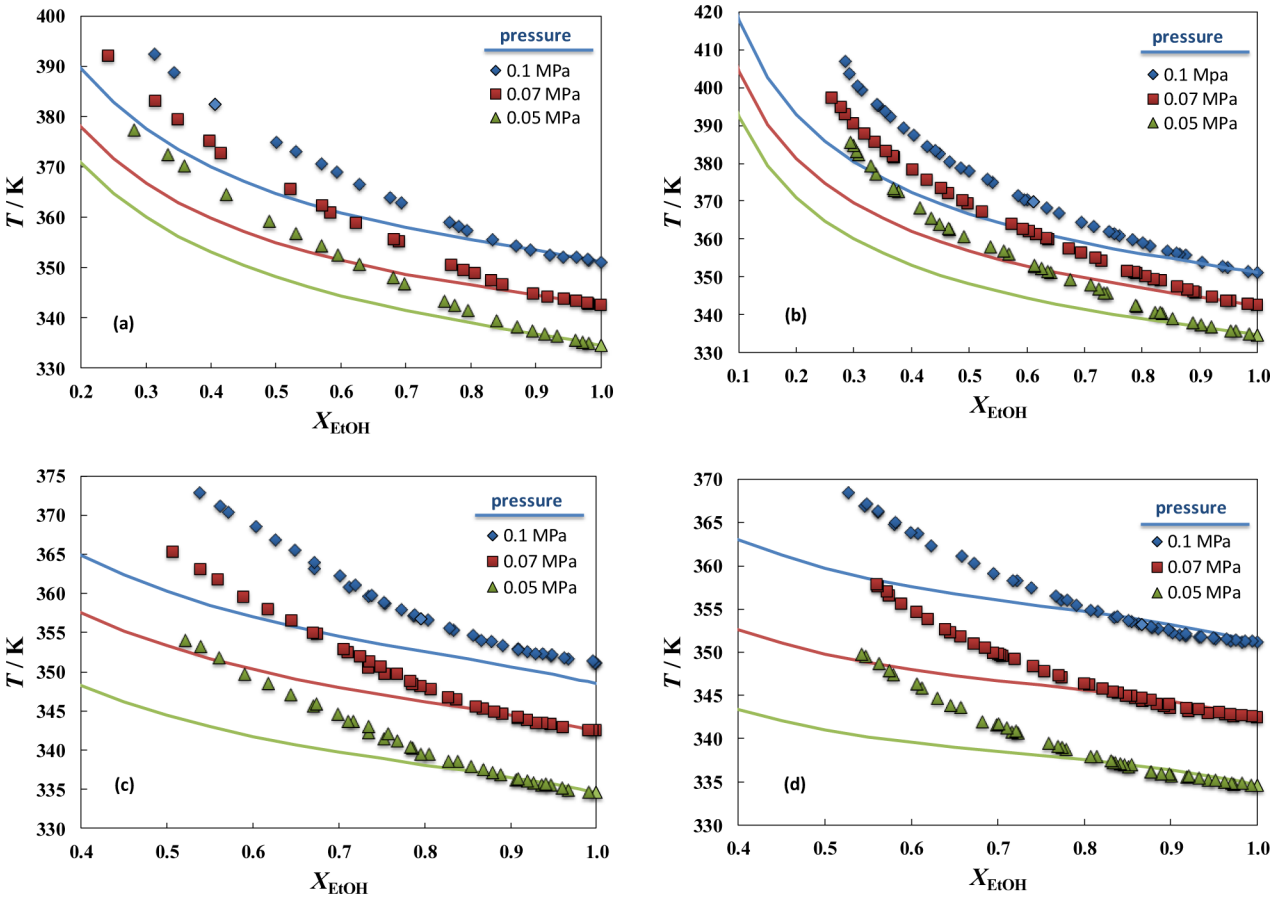

Figure 2. Isobaric temperature−composition diagram of (a) $[C_4C_1im][SCN]$ + ethanol, (b) $[C_4C_1im][N(CN)_2]$ + ethanol, (c) $[C_4C_1im][C(CN)_3]$ + ethanol, and (d) $[C_2C_1im][B(CN)_4]$ + ethanol. The solid lines represent COSMO-RS predictions.

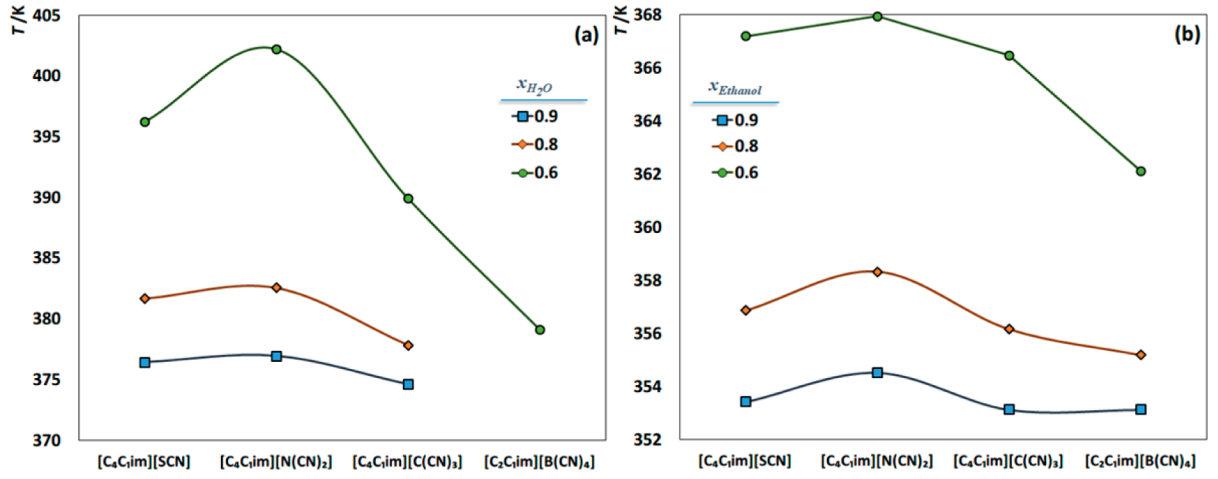

Figure 3. Temperature as a function of the ILs for the systems IL + water (a) and IL + ethanol (b), for the 0.6, 0.8, and 0.9 solute mole fractions and 1 bar.

From the analysis of the Z values obtained for the IL + ethanol interactions, it arises that the highest values are found for the system with the anion $[N(CN)_2]^-$, suggesting more favorable interactions with ethanol, which is in close agreement with the activity coefficients reported in the present study (this was also observed for the aqueous systems with the same ILs). Moreover, with the exception of the anion thiocyanate, the propensity to interact with ethanol suggested from the height of the first peak in the RDFs and by the Z values is $[N(CN)_2]^-$ > $[C(CN)_3]^-$ > $[B(CN)_4]^-$. A similar trend was observed for the aqueous systems, suggesting that an increase of CN-groups in the anion hinders the interaction with polar solvents (water and ethanol), consistent with the nonideality observed in these systems. Additionally, these results are consistent with the CHelpG atomic charges calculated for the nitrogen atoms in the CN groups (the mediators of the interactions between the anion and water or ethanol) which become less negative in the order $[N(CN)_2]^-$ > $[SCN]^-$ > $[C(CN)_3]^-$ > $[B(CN)_4]^-$,

DOI: 10.1021/acs.jpcb.5b03324
J. Phys. Chem. B 2015, 119, 10287−10303

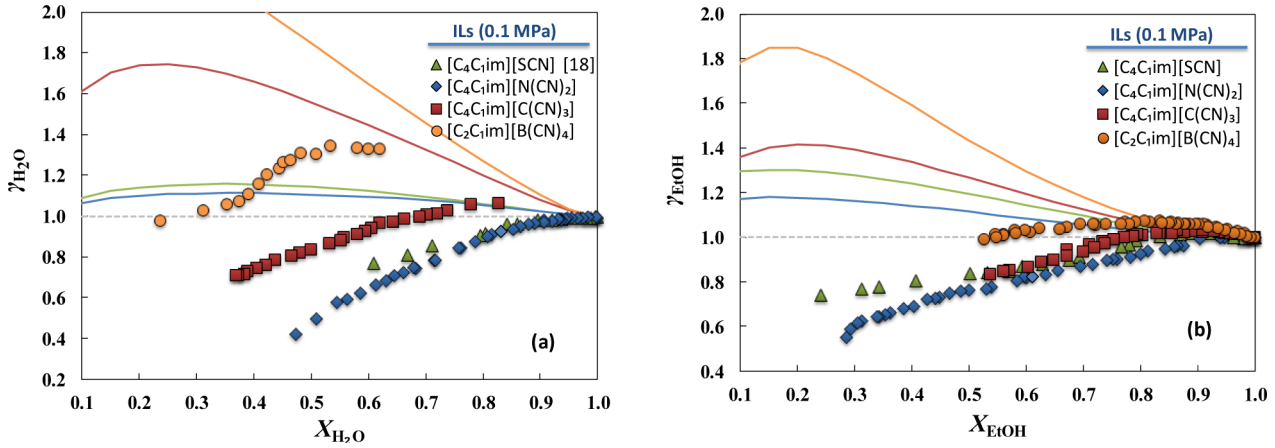

Figure 4. Activity coefficients as a function of water (a) and ethanol (b) mole fractions for the studied systems, at 0.10 MPa. The solid lines represent COSMO-RS predictions.

respectively, with values of −0.723 *e*, −0.658 *e*, −0.638 *e*, and −0.487 *e*.[74] The differences in the CHelpG charges are directly related with the symmetry of the anion and with the presence of different central atoms in each anion, i.e., sulfur ($[SCN]^-$), nitrogen ($[N(CN)_2]^-$), carbon ($[C(CN)_3]^-$) and boron ($[B(CN)_4]^-$), which lead to different charge delocalization, and hence, different abilities of the anions to establish H-bonds with water or ethanol molecules. Remarkably, the ordering of the partial charges in the nitrogen atoms from the CN-groups in the anions of the ILs agrees with the ordering obtained for VLE and activity coefficient information suggesting a strong relationship between the two.

4.2.3. Spatial Distribution Function. To further get a tridimensional visualization of how each anion interacts with ethanol, the spatial distribution functions (SDFs, a 3D representation of the probability of finding a particle at a certain position) were calculated for all considered mixtures and are depicted, by mole fraction of IL, in Figure 6. The SDFs were built and analyzed with the TRAVIS[83] considering only the hydrogen atom from the hydroxyl group of ethanol molecules surrounding each anion of the different ILs considered in this study. Isosurfaces for ethanol (ice blue wired surfaces) with the value of 8 particles·nm^{-3} was considered, at 0.2 mol fraction of IL.

Recognizable for all systems containing ILs, interactions of ethanol with the CN-based anions are established preferentially with the nitrogen atoms of the cyanide groups. This type of interaction was also previously observed for aqueous systems.[74] Nevertheless, the volume of the SDFs for ethanol interacting with the different anions (Figure 6) decreases with the increase of the number of CN-groups in the anion, suggesting that in the case of the anions with less CN-groups, the interaction is more likely to occur, which is consistent with previous findings.

In conclusion, the results from MD simulations suggest that the increase of the number of CN-groups leads to a decrease of interactions with ethanol. This behavior is similar to what was observed for the aqueous systems and supports the nonideality observed in the VLE and the activity coefficients.

5. CONCLUSIONS

Isobaric VLE data for seven water/ethanol + imidazolium based IL systems containing cyano group at three different pressures were measured in this work. The results indicate that the imidazolium-based ILs studied cause boiling-point elevations of different degrees according to the interaction strengths between water/ethanol and the IL. Using the VLE data, activity coefficients were estimated aiming at evaluating the nonideality of the systems considered in this study. The results obtained suggest that, for both water and ethanol systems, the ability of the anions to interact with the solvent decreases with increasing number of cyano groups, with the system containing the anion $[N(CN)_2]^-$ presenting the higher ability to establish favorable interactions. MD simulations were performed for systems composed of ethanol and four different ILs having the common imidazolium-based cation. The MD trajectories were used to calculate radial and spatial distribution functions and also coordination numbers, which were used to infer the nature and profile of the interaction established between ethanol and the ILs. Although presenting slightly different trends, all seem to agree and support the experimental findings, along with activity coefficients data, that an increase of the number of CN-groups in the ILs' anion lead to a decrease in the capability to interact with polar solvents.

■ ASSOCIATED CONTENT

Supporting Information

Isobaric temperature−composition diagrams (Figure S1); activity coefficients as a function of water and ethanol mole fractions (Figure S2); radial and spatial distribution functions (Figure S3); comparison between experimental and simulated density values for different mole fraction of CN-based ILs (Table S1); comparison between experimental and calculated densities and enthalpies of vaporization for of CN-based ILs at 298.15 K (Table S2). The Supporting Information is available free of charge on the ACS Publications website at DOI: 10.1021/acs.jpcb.5b03324.

■ AUTHOR INFORMATION

Corresponding Author

*Telephone: +351 234 401 507. Fax: + 351 234 370 084 E-mail: jcoutinho@ua.pt (J.A.P.C.).

Author Contributions

§Equally contributing authors

Notes

The authors declare no competing financial interest.

DOI: 10.1021/acs.jpcb.5b03324
J. Phys. Chem. B 2015, 119, 10287−10303

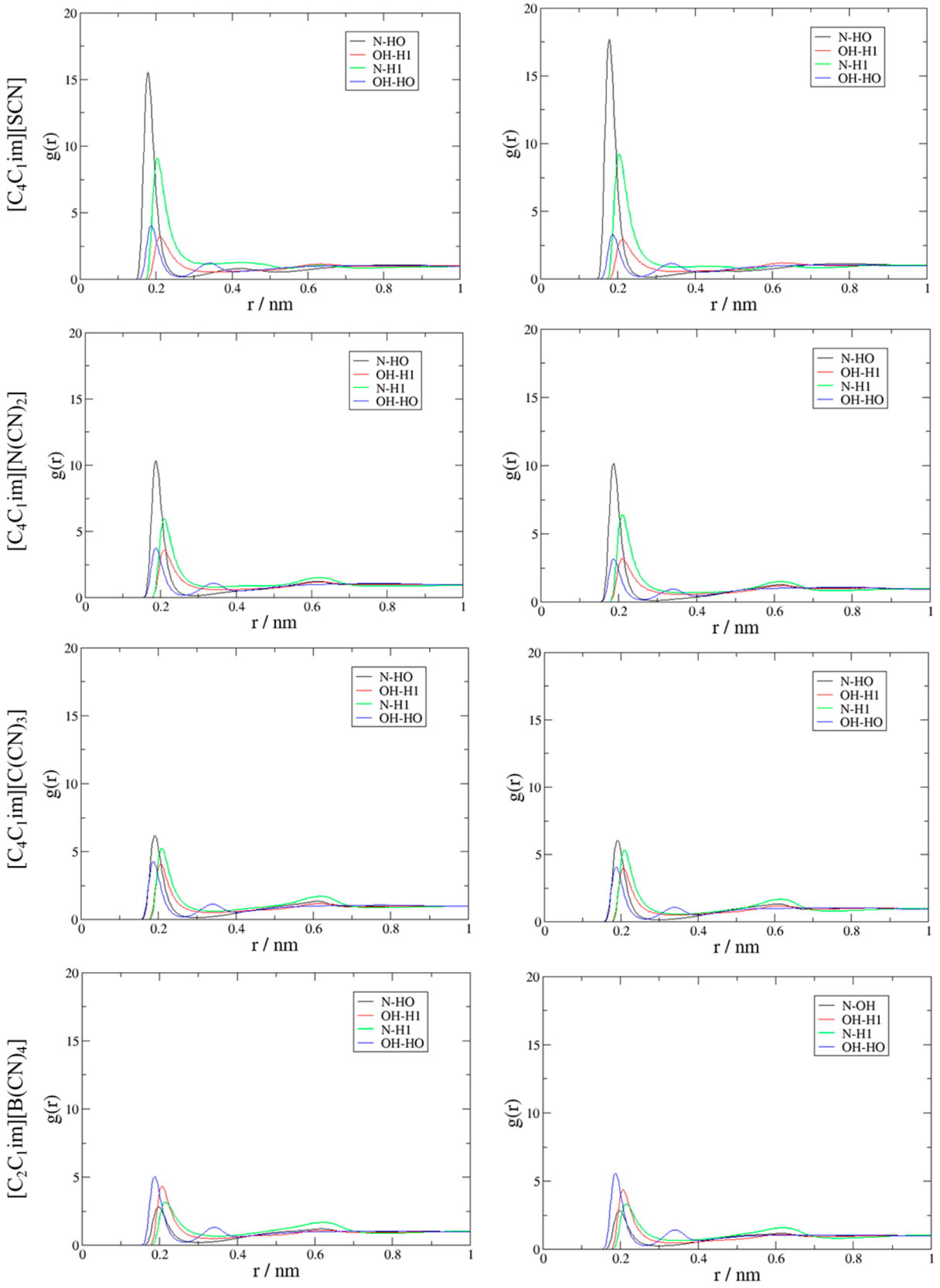

Figure 5. Radial distributions functions (RDFs) for $[C_4C_1im][SCN]$, $[C_4C_1im][N(CN)_2]$, $[C_4C_1im][C(CN)_3]$, and $[C_2C_1im][B(CN)_4]$, at 0.20 (left side) and 0.40 (right side) mole fractions of IL and 298.15 K. In each picture is represented all types of interaction, namely RDFs for anion−ethanol (—), cation−ethanol (red line), cation−anion (green line), and ethanol−ethanol (blue line) interactions.

DOI: 10.1021/acs.jpcb.5b03324
J. Phys. Chem. B 2015, 119, 10287−10303

Table 9. Coordination Numbers (Z) from the RDF Peaks at Distances below r_Z nm, for Anion−Ethanol, Cation−Ethanol, Cation−Anion and Ethanol−Ethanol Interactions, for Each System and at Different IL Mole Fractions

	anion−solvent		cation−solvent		cation−anion		solvent−solvent		IL−solvent
x_{IL}	r_Z	Z	r_Z	Z	r_Z	Z	r_Z	Z	Z(total)
$[C_4C_1im][SCN] + CH_3CH_2OH$									
0.2	0.26	1.44	0.35	1.08	0.35	0.55	0.26	0.46	2.52
0.4	0.26	0.91	0.35	0.57	0.35	0.84	0.26	0.22	1.48
0.6	0.26	0.48	0.35	0.29	0.35	1.04	0.26	0.10	0.77
0.8	0.26	0.20	0.35	0.10	0.35	1.21	0.26	0.03	0.20
$[C_4C_1im][N(CN)_2] + CH_3CH_2OH$									
0.2	0.26	2.08	0.35	1.04	0.35	0.75	0.26	0.41	3.12
0.4	0.26	1.13	0.35	0.55	0.35	1.17	0.26	0.20	1.68
0.6	0.26	0.58	0.35	0.28	0.35	1.39	0.26	0.09	0.86
0.8	0.26	0.23	0.35	0.11	0.35	1.53	0.26	0.02	0.34
$[C_4C_1im][C(CN)_3] + CH_3CH_2OH$									
0.2	0.26	1.95	0.35	0.90	0.35	0.87	0.26	0.43	2.85
0.4	0.26	1.08	0.35	0.50	0.35	1.32	0.26	0.23	1.59
0.6	0.26	0.56	0.35	0.25	0.35	1.57	0.26	0.11	0.81
0.8	0.26	0.23	0.35	0.10	0.35	1.72	0.26	0.05	0.33
$[C_2C_1im][B(CN)_4] + CH_3CH_2OH$									
0.2	0.26	1.54	0.35	0.95	0.35	1.01	0.26	0.53	2.49
0.4	0.26	0.89	0.35	0.53	0.35	1.52	0.26	0.33	1.42
0.6	0.26	0.48	0.35	0.28	0.35	1.82	0.26	0.20	0.77
0.8	0.26	0.21	0.35	0.11	0.35	2.02	0.26	0.09	0.32

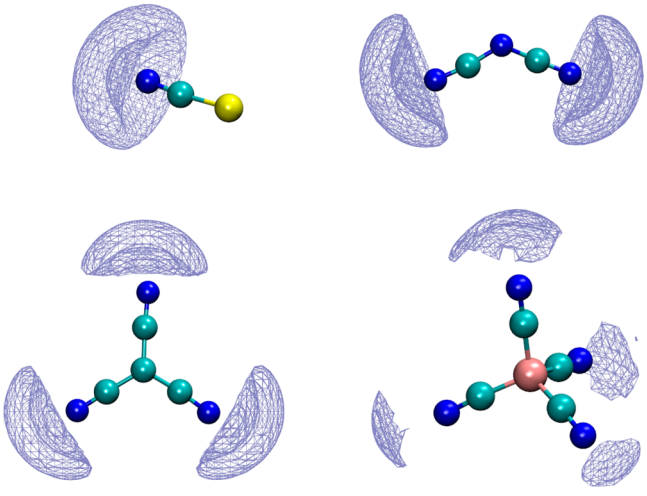

Figure 6. Spatial distribution functions (SDFs) obtained by TRAVIS,[83] for the mixture $[C_4C_1im][SCN]$ (above, left side), $[C_4C_1im][N(CN)_2]$ (above, right side), $[C_4C_1im][C(CN)_3]$ (down, left side), and $[C_2C_1im][B(CN)_4]$ (down, right side) and ethanol, at 0.20 mol fraction of IL. Each anion is the center element, surrounded by hydrogen atoms from the hydroxyl group of ethanol molecules (ice blue wired surface).

■ ACKNOWLEDGMENTS

This work was developed in the scope of the project CICECO−Aveiro Institute of Materials (ref. FCT UID/CTM/50011/2013), financed by national funds through the FCT/MEC and cofinanced by FEDER under the PT2020 Partnership Agreement. The authors thank the Fundação para a Ciência e Tecnologia (FCT) for Programa Investigador FCT and for an exploratory project grant (EXPL/QEQ-PRS/0224/2013). I.K., P.J.C. and M.L.S.B. also acknowledge FCT for the Postdoctoral Grants SFRH/BPD/76850/2011 and SFRH/BPD/82264/2011, and for the Ph.D. Grant SFRH/BD/74551/2010, respectively.

■ REFERENCES

(1) Ge, Y.; Zhang, L.; Yuan, X.; Geng, W.; Ji, J. Selection of Ionic Liquids as Entrainers for Separation of (Water + Ethanol). *J. Chem. Thermodyn.* **2008**, *40*, 1248−1252.
(2) Tsanas, C.; Tzani, A.; Papadopoulos, A.; Detsi, A.; Voutsas, E. Ionic liquids as Entrainers for the Separation of the Ethanol/Water System. *Fluid Phase Equilib.* **2014**, *379*, 148−156.
(3) Lei, Z.; Dai, C.; Zhu, J.; Chen, B. Extractive Distillation with Ionic Liquids: A Review. *AIChE J.* **2014**, *60*, 3312−3329.
(4) Lei, Z.; Li, C.; Chen, B. Extractive Distillation: A Review. *Sep. Purif. Rev.* **2003**, *32*, 121−213.
(5) Pereiro, A. B.; Araújo, J. M. M.; Esperança, J. M. S. S.; Marrucho, I. M.; Rebelo, L. P. N. Ionic Liquids in Separations of Azeotropic Systems − A Review. *J. Chem. Thermodyn.* **2012**, *46*, 2−28.
(6) Vane, L. M. Separation Technologies for the Recovery and Dehydration of Alcohols from Fermentation Broths. *Biofuels, Bioprod. Biorefin.* **2008**, *2*, 553−588.
(7) Huang, H.-J.; Ramaswamy, S.; Tschirner, U. W.; Ramarao, B. V. A Review of Separation Technologies in Current and Future Biorefineries. *Sep. Purif. Technol.* **2008**, *62*, 1−21.

DOI: 10.1021/acs.jpcb.5b03324
J. Phys. Chem. B 2015, 119, 10287−10303

(8) Kirchner, B. *Topics in Current Chemistry*; Springer-Verlag: New York, 2010; Vol. *290*.
(9) Seiler, M.; Jork, C.; Kavarnou, A.; Arlt, W.; Hirsch, R. Separation of Azeotropic Mixtures using Hyperbranched Polymers or Ionic Liquids. *AIChE J.* **2004**, *50*, 2439−2454.
(10) Gutiérrez, J. P.; Meindersma, G. W.; de Haan, A. B. COSMO-RS-based Ionic-Liquid selection for Extractive Distillation Processes. *Ind. Eng. Chem. Res.* **2012**, *51*, 11518−11529.
(11) Jork, C.; Seiler, M.; Beste, Y. A.; Arlt, W. Influence of Ionic Liquids on the Phase behavior of Aqueous Azeotropic Systems. *J. Chem. Eng. Data* **2004**, *49*, 852−857.
(12) Beste, Y.; Eggersmann, M.; Schoenmakers, H. Extractive Distillation with Ionic Fluids. *Chem. Ing. Tech.* **2005**, *77*, 1800−1808.
(13) Lei, Z.; Arlt, W.; Wasserscheid, P. Separation of 1-Hexene and n-Hexane with Ionic Liquids. *Fluid Phase Equilib.* **2006**, *241*, 290−299.
(14) Revelli, A.-L.; Mutelet, F.; Jaubert, J.-N. (Vapor + Liquid) Equilibria of Binary Mixtures Containing Light Alcohols and Ionic Liquids. *J. Chem. Thermodyn.* **2010**, *42*, 177−181.
(15) Carvalho, P. J.; Khan, I.; Morais, A.; Granjo, J. F. O.; Oliveira, N. M. C.; Santos, L. M. N. B. F.; Coutinho, J. A. P. A New Microebulliometer for the Measurement of the Vapor−Liquid Equilibrium of Ionic Liquid Systems. *Fluid Phase Equilib.* **2013**, *354*, 156−165.
(16) Calvar, N.; González, B.; Gómez, E.; Domínguez, Á. Vapor−Liquid Equilibria for the Ternary System Ethanol + Water + 1-Butyl-3-Methylimidazolium Chloride and the corresponding Binary Systems at 101.3 kPa. *J. Chem. Eng. Data* **2006**, *51*, 2178−2181.
(17) Geng, W.; Zhang, L.; Deng, D.; Ge, Y.; Ji, J. Experimental Measurement and Modeling of Vapor−Liquid Equilibrium for the Ternary System Water + Ethanol + 1-Butyl-3-Methylimidazolium Chloride. *J. Chem. Eng. Data* **2010**, *55*, 1679−1683.
(18) Passos, H.; Khan, I.; Mutelet, F.; Oliveira, M. B.; Carvalho, P. J.; Santos, L. M. N. B. F.; Held, C.; Sadowski, G.; Freire, M. G.; Coutinho, J. A. P. Vapor-Liquid Equilibria of Water plus Alkylimidazolium-based Ionic Liquids: Measurements and Perturbed-Chain Statistical Associating Fluid Theory Modeling. *Ind. Eng. Chem. Res.* **2014**, *53*, 3737−3748.
(19) Calvar, N.; González, B.; Gómez, E.; Domínguez, A. Study of the Behaviour of the Azeotropic Mixture Ethanol−Water with Imidazolium-based Ionic Liquids. *Fluid Phase Equilib.* **2007**, *259*, 51−56.
(20) Zhang, L. Z.; Ge, Y.; Ji, D. X.; Ji, J. B. Experimental Measurement and Modeling of Vapor-Liquid Equilibrium for Ternary Systems containing Ionic Liquids: A Case Study for the System Water plus Ethanol+1-Hexyl-3-Methylimidazolium Chloride. *J. Chem. Eng. Data* **2009**, *54*, 2322−2329.
(21) Calvar, N.; Gonzalez, B.; Gomez, E.; Dominguez, A. Vapor-Liquid Equilibria for the Ternary System Ethanol + Water+1-Ethyl-3-Methylimidazolium Ethylsulfate and the corresponding Binary Systems containing the Ionic Lquid at 101.3 KPa. *J. Chem. Eng. Data* **2008**, *53*, 820−825.
(22) Calvar, N.; González, B.; Gómez, E.; Domínguez, A. N. Vapor−Liquid Equilibria for the Ternary System Ethanol + Water + 1-Butyl-3-Methylimidazolium Methylsulfate and the Corresponding Binary Systems at 101.3 kPa. *J. Chem. Eng. Data* **2009**, *54*, 1004−1008.
(23) Calvar, N.; Gómez, E.; González, B. a.; Domínguez, A. n. Experimental Vapor−Liquid Equilibria for the Ternary System Ethanol + Water + 1-Ethyl-3-Methylpyridinium Ethylsulfate and the corresponding Binary Systems at 101.3 kPa: Study of the Effect of the Cation. *J. Chem. Eng. Data* **2010**, *55*, 2786−2791.
(24) Orchillés, A. V.; Miguel, P. J.; Vercher, E.; Martínez-Andreu, A. Using 1-Ethyl-3-Methylimidazolium Trifluoromethanesulfonate as an Entrainer for the Extractive Distillation of Ethanol + Water Mixtures. *J. Chem. Eng. Data* **2010**, *55*, 1669−1674.
(25) Orchilles, A. V.; Miguel, P. J.; Llopis, F. J.; Vercher, E.; Martinez-Andreu, A. Isobaric Vapor-Liquid Equilibria for the Extractive Distillation of Ethanol plus Water Mixtures using 1-Ethyl-3-Methylimidazolium Dicyanamide. *J. Chem. Eng. Data* **2011**, *56*, 4875−4880.
(26) Quijada-Maldonado, E.; Meindersma, G. W.; de Haan, A. B. Ionic Liquid Effects on Mass Transfer Efficiency in Extractive Distillation of Water−Ethanol Mixtures. *Comput. Chem. Eng.* **2014**, *71*, 210−219.
(27) Freire, M. G.; Neves, C. M. S. S.; Marrucho, I. M.; Coutinho, J. A. P.; Fernandes, A. M. Hydrolysis of Tetrafluoroborate and Hexafluorophosphate Counter ions in Imidazolium-based Ionic Liquids. *J. Phys. Chem. A* **2010**, *114*, 3744−3749.
(28) Carvalho, P. J.; Regueira, T.; Santos, L. M. N. B. F.; Fernandez, J.; Coutinho, J. A. P. Effect of Water on the Viscosities and Densities of 1-Butyl-3-Methylimidazolium Dicyanamide and 1-Butyl-3-Methylimidazolium Tricyanomethane at Atmospheric Pressure. *J. Chem. Eng. Data* **2010**, *55*, 645−652.
(29) Nebig, S.; Bolts, R.; Gmehling, J. Measurement of Vapor-Liquid Equilibria (VLE) and Excess Enthalpies (H-F) of Binary Systems with 1-Alkyl-3-Methylimidazolium Bis(trifluoromethylsulfonyl)imide and Prediction of these Properties and gamma(infinity) using Modified UNIFAC (Dortmund). *Fluid Phase Equilib.* **2007**, *258*, 168−178.
(30) García-Sánchez, F.; Eliosa-Jiménez, G.; Silva-Oliver, G.; Vázquez-Román, R. Vapor−Liquid Equilibria of Nitrogen−Hydrocarbon Systems using the PC-SAFT Equation of State. *Fluid Phase Equilib.* **2004**, *217*, 241−253.
(31) Khelassi-Sefaoui, A.; Mutelet, F.; Mokbel, I.; Jose, J.; Negadi, L. Measurement and Correlation of Vapour Pressures of Pyridine and Thiophene with [EMIM][SCN] Ionic Liquid. *J. Chem. Thermodyn.* **2014**, *72*, 134−138.
(32) Freire, M. G.; Santos, L.; Marrucho, I. M.; Coutinho, J. A. P. Evaluation of COSMO-RS for the prediction of LLE and VLE of Alcohols plus Ionic Liquids. *Fluid Phase Equilib.* **2007**, *255*, 167−178.
(33) Verma, V. K.; Banerjee, T. Ionic Liquids as Entrainers for Water + Ethanol, Water + 2-Propanol, and Water + THF Systems: A Quantum Chemical Approach. *J. Chem. Thermodyn.* **2010**, *42*, 909−919.
(34) Dhanalakshmi, J.; Sai, P. S. T.; Balakrishnan, A. R. Study of Ionic Liquids as Entrainers for the Separation of Methyl Acetate−Methanol and Ethyl Acetate−Ethanol systems using the COSMO-RS model. *Ind. Eng. Chem. Res.* **2013**, *52*, 16396−16405.
(35) Freire, M. G.; Ventura, S. P. M.; Santos, L. M. N. B. F.; Marrucho, I. M.; Coutinho, J. A. P. Evaluation of COSMO-RS for the Prediction of LLE and VLE of Water and Ionic Liquids Binary Systems. *Fluid Phase Equilib.* **2008**, *268*, 74−84.
(36) Méndez-Morales, T.; Carrete, J.; Cabeza, O.; Gallego, L. J.; Varela, L. M. Molecular Dynamics Simulations of the Structural and Thermodynamic Properties of Imidazolium-based Ionic Liquid Mixtures. *J. Phys. Chem. B* **2011**, *115*, 11170−11182.
(37) Raabe, G.; Köhler, J. Thermodynamical and Structural Properties of Binary Mixtures of Imidazolium Chloride Ionic Liquids and Alcohols from Molecular Simulation. *J. Chem. Phys.* **2008**, *129*, 144503.
(38) Allen, M. P.; Tildesley, A. K. *Computational Simulations of Liquids.*\; Clarendon Press: Oxford, U.K., 1987.
(39) Batista, M. L. S.; Coutinho, J. A. P.; Gomes, J. R. B. Prediction of Ionic Liquids Properties through Molecular Dynamics Simulations. *Curr. Phys. Chem.* **2014**, *4*, 151−172.
(40) Neves, C. M. S. S.; Kurnia, K. A.; Coutinho, J. A. P.; Marrucho, I. M.; Lopes, J. N. C.; Freire, M. G.; Rebelo, L. P. N. Systematic Study of the Thermophysical properties of Imidazolium-based Ionic Liquids with Cyano-Functionalized Anions. *J. Phys. Chem. B* **2013**, *117*, 10271−10283.
(41) Zhou, D.; Bai, Y.; Zhang, J.; Cai, N.; Su, M.; Wang, Y.; Zhang, M.; Wang, P. Anion Effects in Organic Dye-Sensitized Mesoscopic Solar Cells with Ionic Liquid Electrolytes: Tetracyanoborate Vs Dicyanamide. *J. Phys. Chem. C* **2011**, *115*, 816−822.
(42) Marszalek, M.; Fei, Z.; Zhu, D.-R.; Scopelliti, R.; Dyson, P. J.; Zakeeruddin, S. M.; Grätzel, M. Application of Ionic liquids containing Tricyanomethanide $[C(CN)_3]-$ or tetracyanoborate $[B(CN)_4]-$ anions in Dye-Sensitized Solar Cells. *Inorg. Chem.* **2011**, *50*, 11561−11567.

DOI: 10.1021/acs.jpcb.5b03324
J. Phys. Chem. B 2015, 119, 10287−10303

(43) Cláudio, A. F. M.; Freire, M. G.; Freire, C. S. R.; Silvestre, A. J. D.; Coutinho, J. A. P. Extraction of Vanillin using Ionic-Liquid-based Aqueous Two-Phase Systems. *Sep. Purif. Technol.* **2010**, *75*, 39−47.
(44) Swatloski, R. P.; Spear, S. K.; Holbrey, J. D.; Rogers, R. D. Dissolution of Cellose with Ionic Liquids. *J. Am. Chem. Soc.* **2002**, *124*, 4974−4975.
(45) Zhao, H.; Baker, G. A.; Song, Z.; Olubajo, O.; Crittle, T.; Peters, D. Designing Enzyme-Compatible Ionic Liquids that can Dissolve Carbohydrates. *Green Chem.* **2008**, *10*, 696−705.
(46) Conceicao, L. J. A.; Bogel-Lukasik, E.; Bogel-Lukasik, R. A New Outlook on Solubility of Carbohydrates and Sugar Slcohols in Ionic Liquids. *RSC Adv.* **2012**, *2*, 1846−1855.
(47) Heitmann, S.; Krings, J.; Kreis, P.; Lennert, A.; Pitner, W. R.; Górak, A.; Schulte, M. M. Recovery of n-Butanol using Ionic Liquid-based Pervaporation Membranes. *Sep. Purif. Technol.* **2012**, *97*, 108−114.
(48) Almeida, H. F. D.; Passos, H.; Lopes-da-Silva, J. A.; Fernandes, A. M.; Freire, M. G.; Coutinho, J. A. P. Thermophysical Properties of Five Acetate-based Ionic Liquids. *J. Chem. Eng. Data* **2012**, *57*, 3005−3013.
(49) Bhattacharjee, A.; Varanda, C.; Freire, M. G.; Matted, S.; Santos, L. M. N. B. F.; Marrucho, I. M.; Coutinho, J. A. P. Density and Viscosity Data for Binary Mixtures of 1-Alkyl-3- Methylimidazolium Alkylsulfates + Water. *J. Chem. Eng. Data* **2012**, *57*, 3473−3482.
(50) Batista, M. L. S.; Tomé, L. I. N.; Neves, C. M. S. S.; Gomes, J. R. B.; Coutinho, J. A. P. Characterization of systems of Thiophene and Benzene with Ionic Liquids. *J. Mol. Liq.* **2014**, *192*, 26−31.
(51) Klamt, A.; Schuurmann, G. COSMO: A New Approach to Dielectric Screening in Solvents with Explicit Expressions for the Screening Energy and its Gradient. *J. Chem. Soc., Perkin Trans. 2* **1993**, 799−805.
(52) Klamt, A. *From Quantum Chemistry to Fluid Phase Thermodynamics and Drug Design*; Elsevier: Amsterdam, 2005; pp 1−217.
(53) Kato, R.; Gmehling, J. Systems with Ionic Liquids: Measurement of VLE and γ^{∞} data and Prediction of their Thermodynamic behavior using original UNIFAC, mod. UNIFAC(Do) and COSMO-RS(Ol). *J. Chem. Thermodyn.* **2005**, *37*, 603−619.
(54) Doker, M.; Gmehling, J. Measurement and Prediction of Vapor-Liquid Equilibria of Ternary Systems containing Ionic Liquids. *Fluid Phase Equilib.* **2005**, *227*, 255−266.
(55) Khan, I.; Kurnia, K. A.; Mutelet, F.; Pinho, S. P.; Coutinho, J. A. Probing the Interactions Between Ionic Liquids And Water: Experimental and Quantum Chemical Approach. *J. Phys. Chem. B* **2014**, *118*, 1848−1860.
(56) Khan, I.; Kurnia, K. A.; Sintra, T. E.; Saraiva, J. A.; Pinho, S. P.; Coutinho, J. A. P. Assessing the Activity Coefficients of Water in Cholinium-based Ionic Liquids: Experimental Measurements and COSMO-RS Modeling. *Fluid Phase Equilib.* **2014**, *361*, 16−22.
(57) Reddy, P.; Aslam Siddiqi, M.; Atakan, B.; Diedenhofen, M.; Ramjugernath, D. Activity Coefficients at Infinite Dilution of Organic Solutes in the Ionic Liquid PEG-5 Cocomonium Methylsulfate at T = (313.15, 323.15, 333.15, and 343.15) K: Experimental Results and COSMO-RS predictions. *J. Chem. Thermodyn.* **2013**, *58*, 322−329.
(58) Diedenhofen, M.; Eckert, F.; Klamt, A. Prediction of Infinite Dilution Activity Coefficients of Organic Compounds in Ionic Liquids using COSMO-RS. *J. Chem. Eng. Data* **2003**, *48*, 475−479.
(59) Ferreira, A. R.; Freire, M. G.; Ribeiro, J. C.; Lopes, F. M.; Crespo, J. G.; Coutinho, J. A. P. An Overview of the Liquid−Liquid Equilibria of (Ionic Liquid + Hydrocarbon) Binary Systems and their Modeling by the Conductor-like Screening Model for Real Solvents. *Ind. Eng. Chem. Res.* **2011**, *50*, 5279−5294.
(60) Ferreira, A. R.; Freire, M. G.; Ribeiro, J. C.; Lopes, F. M.; Crespo, J. G.; Coutinho, J. A. P. Overview of the Liquid-Liquid Equilibria of Ternary Systems composed of Ionic Liquid and Aromatic and Aliphatic Hydrocarbons, and their Modeling by COSMO-RS. *Ind. Eng. Chem. Res.* **2012**, *51*, 3483−3507.
(61) Ferreira, A. R.; Freire, M. G.; Ribeiro, J. C.; Lopes, F. M.; Crespo, J. G.; Coutinho, J. A. P. Ionic Liquids for Thiols Desulfurization: Experimental Liquid−Liquid Equilibrium and COSMO-RS description. *Fuel* **2014**, *128*, 314−329.
(62) Diedenhofen, M.; Klamt, A. COSMO-RS as a tool for Property Prediction of IL Mixtures-A Review. *Fluid Phase Equilib.* **2010**, *294*, 31−38.
(63) Hess, B.; Kutzner, C.; van der Spoel, D.; Lindahl, E. GROMACS 4: Algorithms for highly efficient, load-balanced, and scalable molecular simulation. *J. Chem. Theory Comput.* **2008**, *4*, 435−447.
(64) Nosé, S. A Molecular Dynamics Method for Simulations in the Canonical Ensemble. *Mol. Phys.* **1984**, *52*, 255−268.
(65) Hoover, W. G. Canonical Dynamics: Equilibrium Phase-Space Distributions. *Phys. Rev. A: At., Mol., Opt. Phys.* **1985**, *31*, 1695−1697.
(66) Parrinello, M.; Rahman, A. Polymorphic Transitions in Single Crystals: A New Molecular Dynamics Method. *J. Appl. Phys.* **1981**, *52*, 7182−7190.
(67) Batista, M. L. S.; Tomé, L. I. N.; Neves, C. M. S. S.; Rocha, E. M.; Gomes, J. R. B.; Coutinho, J. A. P. The Origin of the LCST on the Liquid−Liquid Equilibrium of Thiophene with Ionic Liquids. *J. Phys. Chem. B* **2012**, *116*, 5985−5992.
(68) Jorgensen, W. L.; Maxwell, D. S.; Tirado-Rives, J. Development and Testing of the OPLS all-Atom Force Field on Conformational Energetics and Properties of Organic Liquids. *J. Am. Chem. Soc.* **1996**, *118*, 11225−11236.
(69) Kaminski, G. A.; Friesner, R. A.; Tirado-Rives, J.; Jorgensen, W. L. Evaluation and Reparametrization of the OPLS-AA Force Field for Proteins via Comparison with Accurate Quantum Chemical Calculations on Peptides. *J. Phys. Chem. B* **2001**, *105*, 6474−6487.
(70) Koller, T.; Ramos, J.; Garrido, N. M.; Fröba, A. P.; Economou, I. G. Development of a United-Atom Force Field for 1-Ethyl-3-Methylimidazolium Tetracyanoborate Ionic Liquid. *Mol. Phys.* **2012**, *110*, 1115−1126.
(71) Breneman, C. M.; Wiberg, K. B. Determining Atom-Centered Monopoles from Molecular Electrostatic Potentials. The need for High Sampling Density in Formamide Conformational Analysis. *J. Comput. Chem.* **1990**, *11*, 361−373.
(72) Becke, A. D. Density-Functional Thermochemistry. III. The Role of Exact Exchange. *J. Chem. Phys.* **1993**, *98*, 5648−5652.
(73) Frisch, M. J.; Trucks, G. W.; Schlegel, H. B.; Scuseria, G. E.; Robb, M. A.; Cheeseman, J. R.; Scalmani, G.; Barone, V.; Mennucci, B.; Petersson, G. A., et al. *Gaussian 09*; Gaussian, Inc.: Wallingford, CT, 2009.
(74) Batista, M. L.; Kurnia, K. A.; Pinho, S. P.; Gomes, J. R.; Coutinho, J. A. Computational and Experimental Study of the Behavior of Cyano-Based Ionic Liquids in Aqueous Solution. *J. Phys. Chem. B* **2015**, *119*, 1567−78.
(75) Kurnia, K. A.; Coutinho, J. A. P. Overview of the Excess Enthalpies of the Binary Mixtures Composed of Molecular Solvents and Ionic Liquids and their Modeling using COSMO-RS. *Ind. Eng. Chem. Res.* **2013**, *52*, 13862−13874.
(76) Królikowska, M. (Solid + Liquid) and (Liquid + Liquid) Phase Equilibria of (IL + Water) Binary Systems. The influence of the Ionic Liquid Structure on Mutual Solubility. *Fluid Phase Equilib.* **2014**, *361*, 273−281.
(77) Cammarata, L.; Kazarian, S. G.; Salter, P. A.; Welton, T. Molecular States of Water in Room Temperature Ionic Liquids. *Phys. Chem. Chem. Phys.* **2001**, *3*, 5192−5200.
(78) Cha, S.; Ao, M.; Sung, W.; Moon, B.; Ahlstrom, B.; Johansson, P.; Ouchi, Y.; Kim, D. Structures of Ionic Liquid-Water Mixtures Investigated by IR and NMR spectroscopy. *Phys. Chem. Chem. Phys.* **2014**, *16*, 9591−9601.
(79) Khan, I.; Taha, M.; Ribeiro-Claro, P.; Pinho, S. P.; Coutinho, J. A. P. Effect of the Cation on the Interactions between Alkyl Methyl Imidazolium Chloride Ionic Liquids and Water. *J. Phys. Chem. B* **2014**, *118*, 10503−14.
(80) *DIPPR 801 Thermophysical Property Database and DIADEM Predictive Software*, version 1.2; AIChE: New York, 2000.
(81) Maginn, E. J. Molecular Simulation of Ionic Liquids: Current Status and Future Opportunities. *J. Phys.: Condens. Matter* **2009**, *21*, 373101.

DOI: 10.1021/acs.jpcb.5b03324
J. Phys. Chem. B 2015, 119, 10287−10303

(82) Skarmoutsos, I.; Dellis, D.; Matthews, R. P.; Welton, T.; Hunt, P. A. Hydrogen Bonding in 1-Butyl- and 1-Ethyl-3-Methylimidazolium Chloride Ionic Liquids. *J. Phys. Chem. B* **2012**, *116*, 4921−4933.
(83) Brehm, M.; Kirchner, B. TRAVIS - A Free Analyzer and Visualizer for Monte Carlo and Molecular Dynamics Trajectories. *J. Chem. Inf. Model.* **2011**, *51*, 2007−2023.

DOI: 10.1021/acs.jpcb.5b03324
J. Phys. Chem. B 2015, 119, 10287−10303